Magnetic moments, exchange coupling, and crossover temperatures of Co clusters on Pt(111) and Au(111)

2007 J. Phys.: Condens. Matter 19 096203

(http://iopscience.iop.org/0953-8984/19/9/096203)

IOP PUBLISHING JOURNAL OF PHYSICS: CONDENSED MATTER

J. Phys.: Condens. Matter **19** (2007) 096203 (21pp) doi:10.1088/0953-8984/19/9/096203

Magnetic moments, exchange coupling, and crossover temperatures of Co clusters on Pt(111) and Au(111)

O Šipr[1], S Bornemann[2], J Minár[2], S Polesya[2], V Popescu[2,3], A Šimůnek[1] and H Ebert[2]

[1] Institute of Physics, Academy of Sciences of the Czech Republic, Cukrovarnická 10, CZ-162 53 Prague, Czech Republic
[2] Universität München, Department Chemie, Butenandtstraße 5-13, D-81377 München, Germany

E-mail: sipr@fzu.cz and Hubert.Ebert@cup.uni-muenchen.de

Received 20 November 2006, in final form 22 December 2006
Published 14 February 2007
Online at stacks.iop.org/JPhysCM/19/096203

Abstract

The influence of cluster size and of cluster–substrate interaction on the magnetic properties of Co clusters of 1–10 atoms on Pt(111) and Au(111) is studied by fully relativistic *ab initio* calculations. The focus is on systematic trends of the spin and orbital magnetic moments, the exchange coupling, and the crossover temperature. The spin magnetic moments of Co clusters are larger for the Pt substrate than for the Au substrate, while the reverse is true for the orbital magnetic moments. The local magnetic moments of Co atoms generally increase if the number of Co neighbours decreases. The exchange coupling constants J_{ij} depend on the cluster size and on the location of respective atoms. The crossover temperature increases monotonically with cluster size and is larger for clusters on Pt than for clusters on Au.

(Some figures in this article are in colour only in the electronic version)

1. Introduction

Metallic clusters have been the focus of intensive basic as well as applied research recently. From a fundamental point of view, clusters offer the possibility to study the evolution of physical and chemical properties from atoms to nanostructures to solids. They contain a large portion of surface atoms, yet their properties cannot be expressed as a mere linear combination of surface and bulk contributions; finite cluster dimensions and associated quantum size effects are significant factors as well. From an application point of view, clusters are promising in many technological fields, including high-density magnetic recording, spintronics, or bio-magnetic sensors.

[3] Present address: Max-Planck-Institut für Metallforschung, Heisenbergstraße 3, D-70569 Stuttgart, Germany.

Recent advances in nanostructure technology made it possible to prepare supported clusters with sizes reaching down to several atoms. For experimental investigations of supported clusters, x-ray magnetic circular dichroism (XMCD) has proved to be an extremely powerful tool as it allows one to measure local spin and orbital magnetic moments in an element-specific way [1, 2]. While first experimental work was done on rather large clusters [1, 3], it is now also possible to study very small clusters consisting of only a few atoms [4–6]. These experiments showed that both the spin magnetic moment $\mu_{\rm spin}$ and the orbital magnetic moment $\mu_{\rm orb}$ of small clusters are strongly enhanced with respect to the bulk.

Theoretical studies focused on overlayers and ad-atoms initially. Recently, a number of theoretical investigations on deposited clusters have been performed as well. These have been done mostly in a non-relativistic or scalar-relativistic way, relying either on spin density functional theory or on parameterized tight-binding model Hamiltonians [7–10]. Several studies also included the influence of spin–orbit coupling, thus giving access to orbital magnetic moments and magnetocrystalline anisotropy [11–14]. On the other hand, very little attention was paid to the exchange coupling between local magnetic moments in supported clusters and to the associated question of thermal stability of the cluster magnetism.

The purpose of our work is to study the influence of the cluster size and of the substrate–cluster interaction on magnetic moments, exchange coupling, and crossover temperatures of supported clusters. We focus on Co clusters of up to ten atoms supported by Pt(111) and by Au(111). This choice is motivated by the availability of relevant experiments [6, 15–17] and by the fact that Pt and Au appear to behave differently when interfaced with a magnetic material [18–20]. Our theoretical framework is based on a material-specific *ab initio* approach, with no adjustable parameters. Both the clusters and the substrate are treated fully relativistically, on the same footing. In order to separate the influence of the geometry and of the electronic structure, we investigate also a third substrate: namely, a hypothetical fcc Au with the lattice parameter of Pt.

The outline of the paper is the following. First we describe our theoretical framework, then we present results for $\mu_{\rm spin}$ and $\mu_{\rm orb}$ of Co clusters and investigate how they depend on the coordination numbers. This is followed by studying the size dependence of magnetic moments of clusters on different substrates. The density of states for different substrates and for different cluster sizes is shown afterwards. The subsequent section is devoted to the exchange coupling in Co clusters and to the way it depends on local magnetic moments and coordination of individual atoms and on the substrate. Finally, the crossover temperature of the various systems is investigated.

2. Computational scheme

Zero-temperature properties of supported clusters were calculated within the *ab initio* spin density functional theory, relying on the local spin density approximation (LSDA). The Vosko, Wilk, and Nusair parameterization of the corresponding exchange and correlation potential was used [21]. The electronic structure is described, including all relativistic effects, by the corresponding Dirac equation. Our approach to solve it is based on the spin-polarized relativistic multiple-scattering or Korringa–Kohn–Rostoker (SPR-KKR) formalism [22, 23], implemented in two steps. In the first step, the Green's function of a clean surface (a 'host') is calculated by applying the tight-binding computational scheme [24]. In the second step, the supported clusters are treated as a perturbation to the clean surface and the Green's function of the new system is obtained self-consistently by solving the Dyson equation. A more detailed description of this procedure can be found in our earlier papers [14, 25].

In all our calculations, we assume that the atoms are located on ideal lattice sites of the underlying bulk fcc lattice. The vacuum region is represented by layers of empty sites. Two

ways of modelling the clean surface were used: either by a slab of 18 metallic layers topped by 6 vacuum layers or by two half-crystals separated by 18 vacuum layers, with electronic structure allowed to relax within 12 metallic layers of each of the half-crystals. We found that these models are practically equivalent (the magnetic moments of deposited Co atoms calculated by both approaches differ by less than 0.01 μ_{B}). One has to bear in mind that, because of our neglect of the structure relaxation, the results contain a systematic deviation with respect to experiment. The distance of Co atoms from the substrate as well as the Co interatomic distances get shorter if structure relaxation is taken into account [26]. On the other hand, by fixing the geometry, we proceed in our study along a well-defined direction; we isolate the net effect of varying the cluster size and can observe how the transition from clusters to overlayers to the bulk affects the magnetic properties.

When solving the Dyson equation for the perturbed systems, impurity clusters of 87 sites were used. This size is fully sufficient: we checked that if only 55 atoms were included, the resulting magnetic moments changed by less than 0.01 μ_{B}. The direction of the magnetization for $T = 0$ K was fixed perpendicular to the (111) crystal surface. The effective potentials were treated within the atomic sphere approximation (ASA). For the multipole expansion of the Green's function, an angular momentum cutoff of $\ell_{\max} = 2$ was used. For selected systems (Co_1, Co_2, and Co_4 clusters and a complete Co overlayer) we performed the calculations also for $\ell_{\max} = 3$ and found that this causes an increase of the local spin moment μ_{spin} by 3–5% and an increase of the local orbital moment μ_{orb} by 3–10%. This indicates that the systematic trends in μ_{spin} and μ_{orb} are well described by $\ell_{\max} = 2$.

The spherically symmetric ASA potential was constructed by including a full charge density in the atomic spheres, using a multipole expansion up to $2\ell_{\max}$. It was demonstrated that this procedure eliminates most of the deficiencies of the shape approximation to the potential at metallic surfaces, unless one is interested in truly vacuum states [27]. Likewise, it was shown recently that ASA potentials are appropriate for describing spectroscopic properties of free noble metal clusters [28].

Investigations of magnetic properties at finite temperatures were based on calculating the ground-state electronic structure in a scalar-relativistic way, considering only the spin magnetic moments. We assume that the energetics connected with the deviation of spins from a ferromagnetic order can be described by a classical Heisenberg spin Hamiltonian,

$$H_{\mathrm{eff}} = -\sum_{i \neq j} J_{ij}\, \boldsymbol{e}_i \cdot \boldsymbol{e}_j, \tag{1}$$

where J_{ij} is the exchange coupling constant between atoms i and j and $\boldsymbol{e}_i$, $\boldsymbol{e}_j$ are unit vectors pointing in the directions of the corresponding local magnetic moments. For mapping of the *ab initio* results onto the Heisenberg model, we rely on the formula of Liechtenstein *et al* [29],

$$J_{ij} = -\frac{1}{4\pi}\,\mathrm{Im}\int^{E_{\mathrm{F}}} \mathrm{d}E\ \mathrm{Tr}(t_{i\uparrow}^{-1} - t_{i\downarrow}^{-1})\,\tau_{\uparrow}^{ij}\,(t_{j\uparrow}^{-1} - t_{j\downarrow}^{-1})\,\tau_{\downarrow}^{ji}, \tag{2}$$

which was derived by exploiting the multiple-scattering formalism, linear response theory, the spin-polarized local force theorem, and the long-wave approximation.

The expectation value of an observable A as a function of spin directions, $A(\{\boldsymbol{e}_i\})$, can be written as

$$\langle A \rangle = \frac{\mathrm{Tr}\exp(-H_{\mathrm{eff}}/kT)\,A}{\mathrm{Tr}\exp(-H_{\mathrm{eff}}/kT)}. \tag{3}$$

We evaluated (3) by a Monte Carlo (MC) method [30] using the standard Metropolis importance sampling algorithm [31]. The J_{ij}-values obtained from (2) were taken as input parameters. For each temperature, about 10^7–10^8 MC steps per atom were performed; the simulation started

from a collinear orientation of all atomic magnetic moments and each step consisted of a random rotation of the spin directions. In that way, the magnetization M of clusters as a function of the temperature T can be obtained as the expectation value of cluster magnetic moments. A similar procedure was applied recently in our study of free clusters [32].

Unlike in the case of crystals, no clear-cut magnetic transition temperature can be defined for clusters because well-defined phase transitions do not occur in finite systems. However, the $M(T)$ curve exhibits an inflection point for a finite system and the corresponding temperature can thus be identified as the crossover temperature T_c. Another way of defining T_c is to associate it with the change of the internal energy which occurs when the system transits from a dominantly ordered to a dominantly disordered state. The crossover temperature is then taken as the position of a peak in the specific heat as a function of the temperature. We used this second definition of T_c here, because for very small clusters, a peak in the specific heat is a significantly more distinguished feature than an inflection point of the $M(T)$ curve. However, temperatures determined in both ways to not differ very much from one another and the final picture does not depend on the choice of the definition of T_c. Finally, it should be noted that T_c obtained this way would not change significantly if magnetic anisotropy were included in the Hamiltonian (1) in a realistic way [14].

3. Results and discussion

3.1. Local magnetic moments

Calculated values of local μ_{spin} and μ_{orb} for Co clusters of 1–7 atoms supported by the Pt(111) surface are displayed in figures 1 and 2; analogous data for clusters supported by the Au(111) surface are displayed in figures 3 and 4. Figure 1 also shows μ_{spin} induced in the Pt substrate. Our results for bilayer clusters of 10 atoms are shown in figure 5; in this case, magnetic moments induced in the atoms below the clusters are shown for both substrates. One can see that there is sometimes a considerable variation of μ_{spin} and μ_{orb} between different sites of the same cluster. Sites with a lower coordination number generally have larger μ_{spin} and μ_{orb} than sites with a higher coordination number. Clusters supported by Pt have larger μ_{spin} than clusters supported by Au, while the reverse is true for μ_{orb}. Note that, because of the presence of Co clusters, substrate atoms which belong to the same layer are in general not equivalent any more—the symmetry is reduced. This reduction of symmetry leads, for example, to an 8% difference between μ_{orb} of atoms at the left and right edges of the Co_5 cluster on Au (see centre of figure 4).

There is a big difference between induced magnetic moments in the Pt and in the Au substrates. Pt atoms which are nearest neighbours of any Co atom have a relatively large μ_{spin} of 0.07–0.14 μ_B, while analogous Au atoms have a small *negative* μ_{spin}, not larger than 0.02 μ_B in absolute value. Substrate atoms with a larger number of Co neighbours usually have a larger μ_{spin} than substrate atoms with a smaller number of Co neighbours. However, this is not a general rule (cf atoms below the central atom of the cross-shaped Co_5 cluster in figure 1). The orbital magnetic moment induced in the substrate atoms is always small: it is less than 0.03 μ_B for Pt and practically zero for Au (less than 0.002 μ_B in absolute value). The fact that Pt atoms are much more polarizable than Au atoms is consistent with earlier theoretical [18] as well as experimental studies [19, 20], and can be related to the high spin susceptibility of Pt due to the large density of states at the Fermi level.

Local magnetic moments in some Co clusters on Pt(111) can be compared with earlier studies based on a similar theoretical approach. For a linear Co_3 cluster, Lazarovits *et al* [33] found $\mu_{spin} = 2.15\ \mu_B$ and $\mu_{orb} = 0.38\ \mu_B$ at the edge atom and $\mu_{spin} = 2.12\ \mu_B$ and

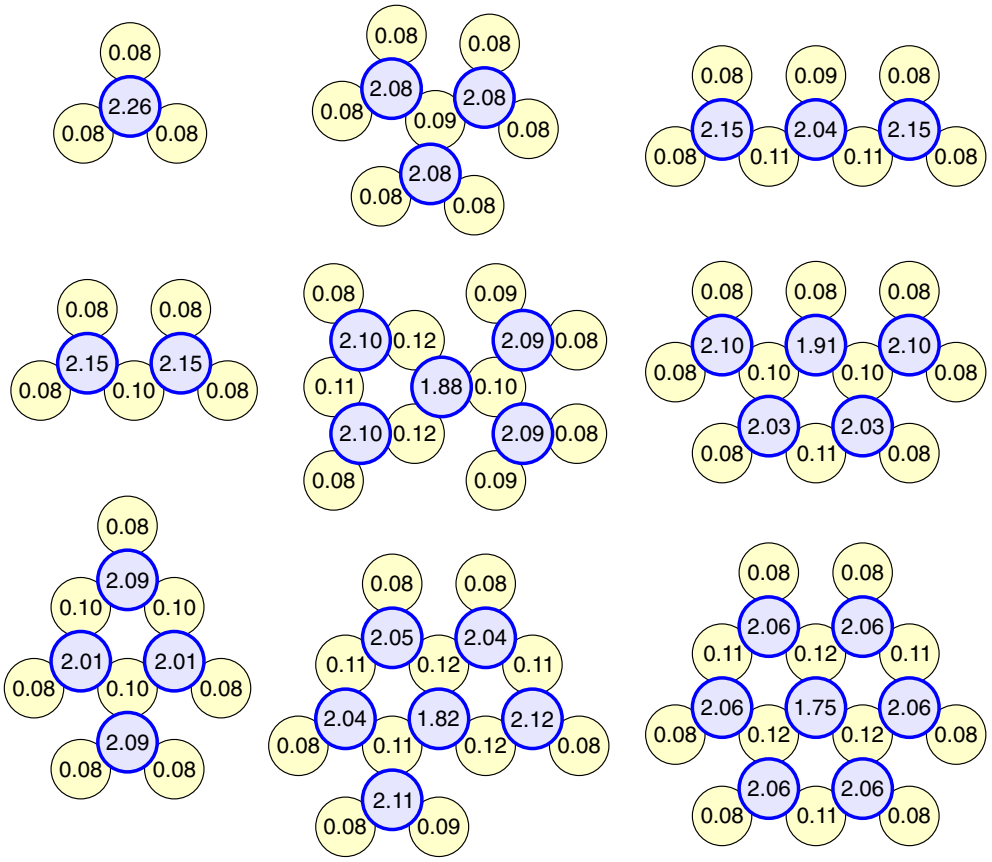

Figure 1. Local μ_{spin} at Co atoms and at substrate atoms for Co clusters of 1–7 atoms supported by Pt(111). Only those substrate atoms which are nearest neighbours of any Co atom are shown.

$\mu_{\mathrm{orb}} = 0.36\ \mu_{\mathrm{B}}$ at the central atom; the site dependence is thus slightly more pronounced in our calculations. Gambardella *et al* [6] presented results for the local orbital moment μ_{orb} for a linear Co_3 cluster, for a Co_4 cluster and for a cross-shaped Co_5 cluster. A direct comparison of their and our results is not possible because the calculations of Gambardella *et al* included the so-called orbital polarization (OP) [12, 34], which we did not consider. In order to have an estimates of how the local μ_{orb} of these authors would look like without OP, we assume that including OP increases μ_{orb} for all atoms in a cluster by the same factor. Under this assumption, such a factor can be determined by employing the total μ_{orb} of the clusters as calculated with OP and without it, which were published in [6]. The ratio of both values provides the factor we need. In that way, we estimate that, without OP, the local μ_{orb} of Gambardella *et al* [6] would be the following: $0.36\ \mu_{\mathrm{B}}$ at the edge atoms and $0.30\ \mu_{\mathrm{B}}$ at central atom of the linear Co_3 cluster, $0.25\ \mu_{\mathrm{B}}$ at the acute-angle atoms and $0.19\ \mu_{\mathrm{B}}$ at the obtuse-angle atoms of the Co_4 cluster, and $0.29\ \mu_{\mathrm{B}}$ at the corner atoms and $0.20\ \mu_{\mathrm{B}}$ at the central atom of the cross-shaped Co_5 cluster. These values are in a very good agreement with our values presented in figure 2.

One can quantify the site dependence of the magnetic moments by plotting μ_{spin} and μ_{orb} as functions of the coordination number. Figure 6 shows such graphs for the Pt substrate, while figure 7 shows the same for the Au substrate. Only Co atoms are considered when defining the coordination number of each site. Results for a Co overlayer on Pt(111) and on Au(111) are also

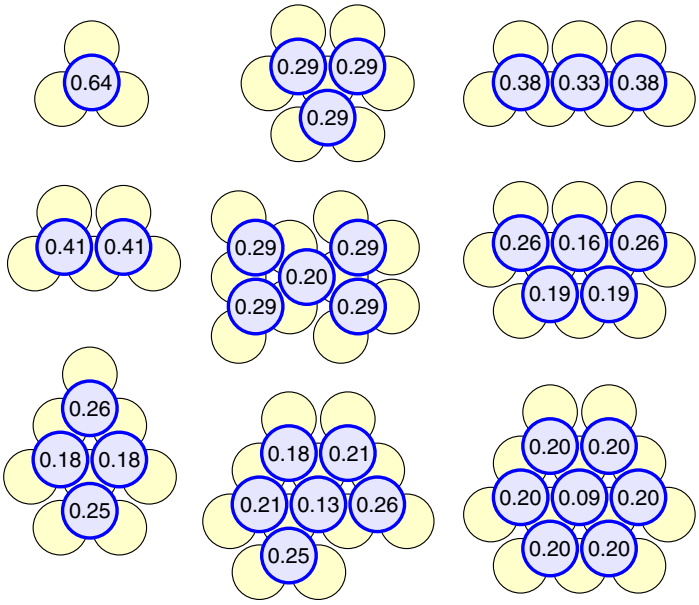

Figure 2. Local μ_{orb} at Co atoms for clusters of 1–7 atoms on Pt(111).

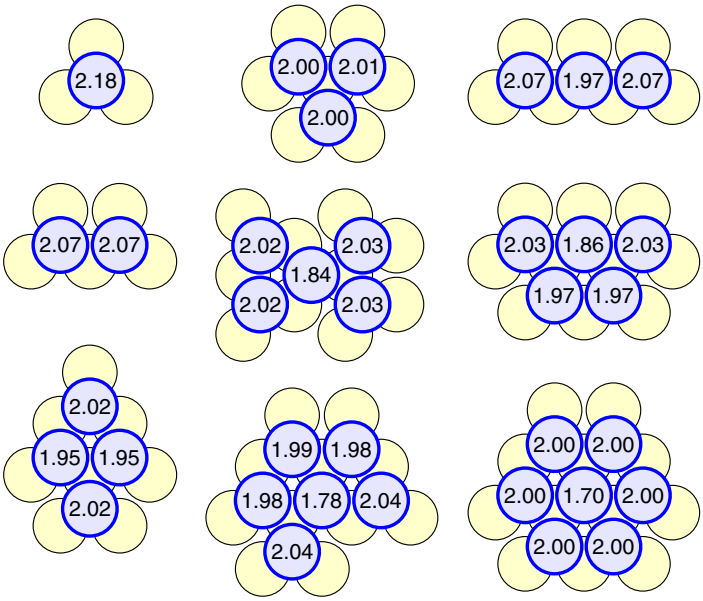

Figure 3. Local μ_{spin} at Co atoms for clusters of 1–7 atoms on Au(111).

shown for comparison. A quasilinear correlation between μ_{spin} and coordination numbers can be found for clusters of 1–7 atoms. The data for a bilayer 10-atom cluster and for an overlayer do not quite fit into this correlation—although the general trend that μ_{spin} and μ_{orb} increase with decreasing coordination number is valid also for these systems. The relation between μ_{spin} and coordination numbers was demonstrated earlier for free Fe clusters and surfaces [35] and for

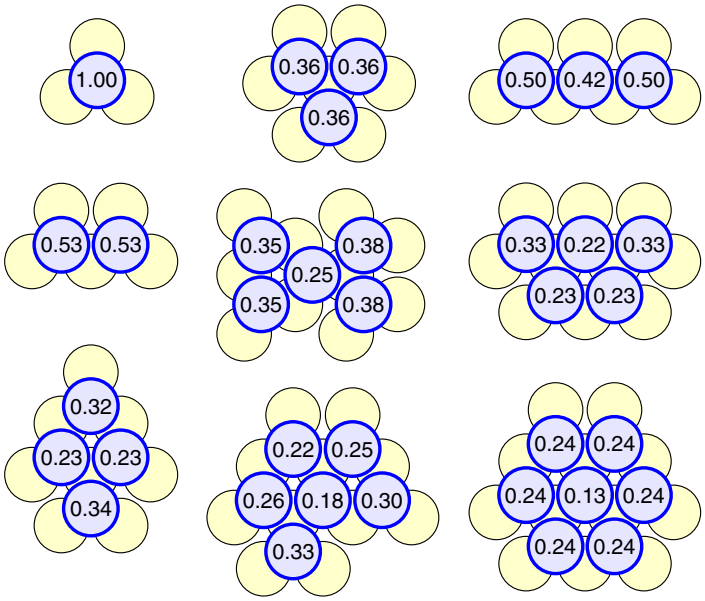

Figure 4. Local μ_{orb} at Co atoms for clusters of 1–7 atoms on Au(111).

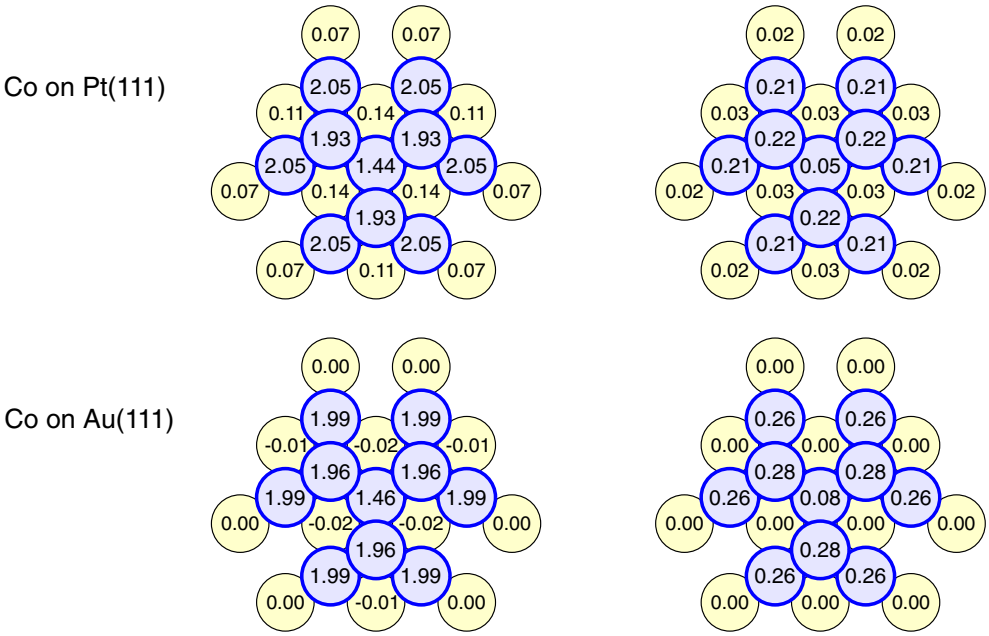

Figure 5. Local μ_{spin} (left diagrams) and μ_{orb} (right diagrams) of Co atoms and of substrate atoms for bilayer 10-atom clusters on Pt (upper diagrams) and on Au (lower diagrams).

supported Fe clusters [13, 36]. Obviously, it could be used to estimate the magnetic moments of clusters too large to be handled by current theoretical and computational means.

The right graphs of figures 6 and 7 demonstrate also a steep and essentially monotonic decrease of μ_{orb} with the coordination number. This dependence, however, cannot be

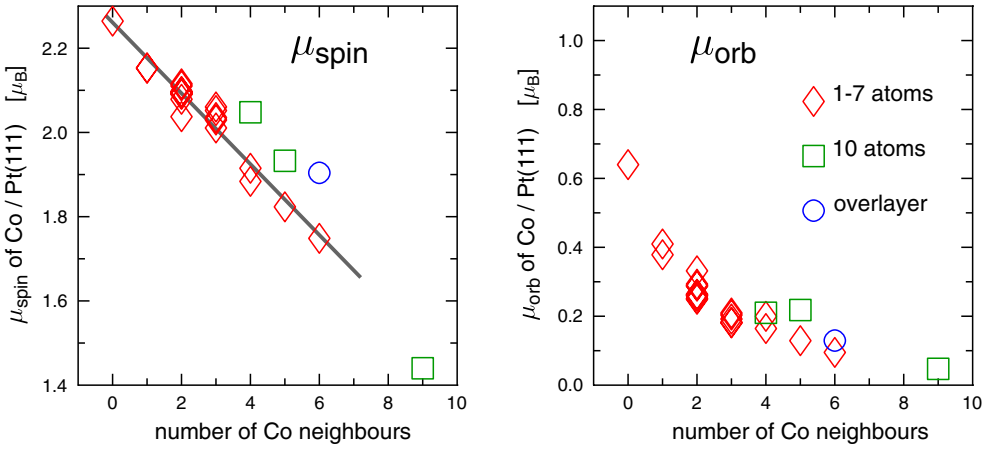

Figure 6. Local μ_{spin} and μ_{orb} of atoms in Co clusters on Pt(111) plotted against the number of Co neighbours of these atoms. Data for monolayer clusters of 1–7 atoms are shown by diamonds; data for the bilayer cluster of 10 atoms are shown by squares. The corresponding value for a complete Co overlayer on Pt is shown by a circle. The line is a least-squares fit to the data for clusters of 1–7 atoms.

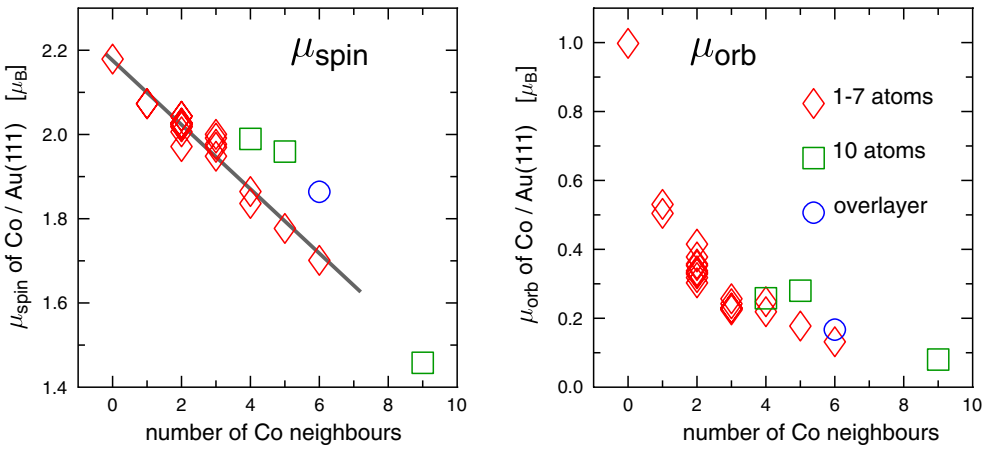

Figure 7. Local μ_{spin} and μ_{orb} of atoms in Co clusters on Au(111) plotted against the number of Co neighbours of these atoms. This plot is analogous to figure 6.

approximated by a simple linear function, and the relative spread of μ_{orb}-values for a given coordination number is larger than in the case of μ_{spin}. The strong dependence of μ_{orb} on the coordination number was observed earlier for Fe clusters on the Ag(001) surface [37] and for free Fe clusters as well [35].

One has to ask how the overall picture would change if structural relaxations were included. This can be estimated by observing the effect of structural relaxations on magnetic moments of Co_1 and Co_9 clusters on Cu(001) [38] and of a monatomic Co wire on Pt(997) [39, 40]. It follows from these studies that Co–Pt distances would decrease by up to 13%, μ_{spin} would decrease by 3–10% and μ_{orb} would decrease by 20–30%. For substrate atoms, the induced magnetic moments would increase (in the case of a Co wire on Pt, the induced μ_{spin} increases by 0.05–0.10 μ_B while the induced μ_{orb} remains practically unchanged [39, 40]). The

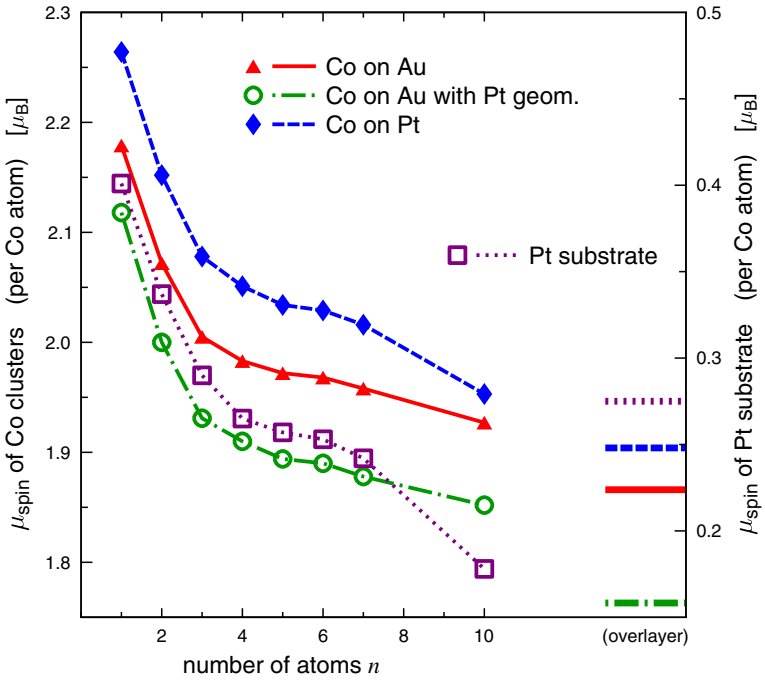

Figure 8. Average μ_{spin} of compact Co clusters of 1–10 atoms on Au, on Au with Pt geometry, and on Pt is shown in the scale of the left vertical axis. The right vertical axis defines the scale of μ_{spin} induced in the Pt substrate. Corresponding values for Co overlayers and for the Pt substrate below a Co overlayer are indicated by horizontal lines at the right border of the graph.

effect of structural relaxation would be more pronounced for ad-atoms than for larger clusters. Importantly, the changes caused by structural relaxation are all in the same direction (this was observed also for Co clusters embedded in a surface [41] or in the bulk [42]). Therefore, one can expect that including structural relaxations in our study would lead to quantitative but not qualitative changes, and that the systematic trends would be the same.

3.2. Size dependence of average magnetic moments

In this section we investigate the dependence of μ_{spin} and μ_{orb} on the cluster size. The total μ_{spin} per Co atom for clusters supported by (111) surfaces is shown in figure 8; the total μ_{orb} per Co atom is shown in figure 9. Only compact cluster shapes are considered, i.e., the Co_3 cluster is of a triangular shape and the Co_5 cluster is of a half-moon shape. The substrates now include not only Pt and Au but also a hypothetical Au with the geometry of Pt. The total magnetic moment induced in the Pt substrate (per Co atom) is also displayed; the magnetic moments induced in the Au substrate are too small and are not shown. For comparison, the magnetic moments for Co overlayers on all three substrates are shown as well. Figure 9 includes also experimental values of μ_{orb} for small Co clusters and for a Co overlayer on Pt(111) deduced by Gambardella *et al* [6] by applying the sum rules to their XMCD spectra.

Clusters supported by Pt(111) have a larger μ_{spin} than clusters on Au(111)—typically by 0.06–0.07 μ_B. This difference would be about twice as large if the lattice constants of the substrates were the same: if the Au lattice constant of 7.71 au is decreased to the Pt value of 7.39 au, μ_{spin} of Co clusters decreases (see figure 8). Such a decrease is in agreement

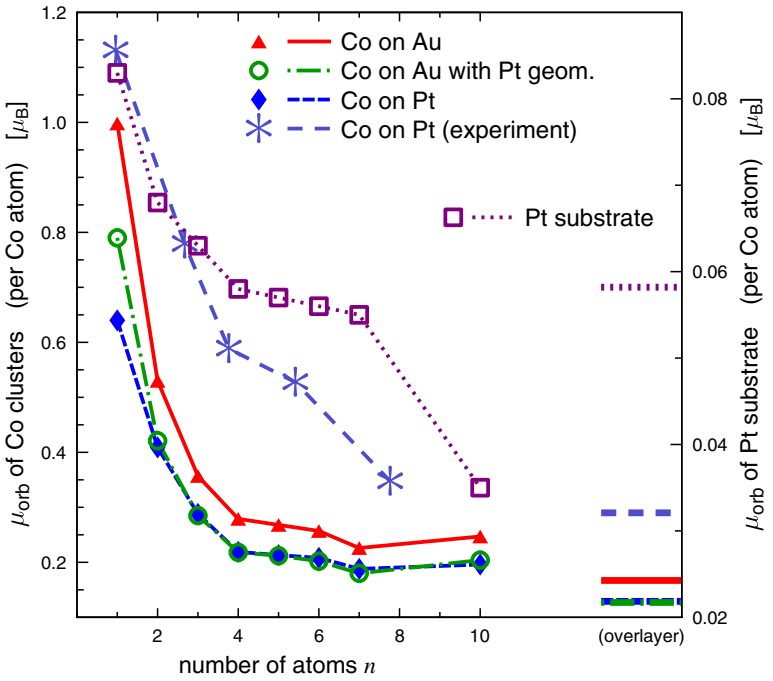

Figure 9. Average μ_{orb} of compact Co clusters of 1–10 atoms on Au, on Au with Pt geometry, and on Pt is shown in the scale of the left vertical axis. The right vertical axis defines the scale of μ_{orb} induced in the Pt substrate below the Co clusters. Corresponding values for Co overlayers are indicated at the right border. Experimental data for Co_n clusters and for a Co overlayer on Pt are shown as well [6]. Note that the theoretical data for Co_n on Au with Pt geometry and for Co_n on Pt nearly coincide for $n \geqslant 2$.

with intuitive expectation: smaller interatomic distances generally lead to smaller magnetic moments. The fact that clusters on Pt have larger μ_{spin} than clusters on Au means that the electronic structure effects more than outbalance the effect of the lattice compression. On the other hand, the orbital magnetic moments are larger for clusters on Au(111) than for clusters on Pt(111). It follows from figure 9 that in this case the difference between Au and Pt substrates could be attributed to the difference in lattice constants alone: the data points for Pt and for Au with Pt geometry nearly coincide for clusters of two or more atoms and for an overlayer.

Magnetic moments of overlayers can be seen as asymptotic values for monolayer clusters Co_n if $n \to \infty$. Our results for all three substrates are consistent in this respect. Magnetic moments of bulk systems are even lower. For a hypothetical bulk Co with an fcc lattice of Pt we obtain $\mu_{spin} = 1.81\ \mu_B$ and $\mu_{orb} = 0.14\ \mu_B$; for bulk Co with an fcc lattice of Au we obtain $\mu_{spin} = 1.89\ \mu_B$ and $\mu_{orb} = 0.17\ \mu_B$.

Comparison of our results with earlier theoretical investigations of Co clusters [6, 33] and of a Co overlayer [33, 43, 44] on Pt(111) with the same geometry as investigated here is done in tables 1 and 2. There is a good agreement in most cases. Spin magnetic moments calculated in this work exhibit a larger variation with cluster size and shape than the moments obtained by Gambardella *et al* [6]. A possible cause of this difference may be a different treatment of the Pt host in both calculations: we treat it fully relativistically while Gambardella *et al* treat it in a scalar-relativistic way [45].

Another comparison can be made with the results of Sabiryanov *et al* [26] who performed non-relativistic full-potential calculations of Co_1, Co_2, and triangular Co_3 clusters on Pt(111)

Table 1. μ_{spin} of Co clusters (per atom) and of a Co overlayer on Pt(111) calculated in this work compared to results of other calculations. The unit is μ_B.

	This work	[6]	[33]	[43]	[44]
Co_1	2.26	2.14	2.21		
Co_2	2.15	2.11	2.17		
Co_3 triangle	2.08	2.10			
Co_3 linear	2.12	2.08	2.14		
Co_4	2.05	2.08			
Co_5 cross	2.05	2.08			
Overlayer	1.90		2.00	1.89	2.00

Table 2. μ_{orb} of Co clusters (per atom) and of a Co overlayer on Pt(111) calculated in this work compared to results of other calculations. The results of [6] are those obtained without OP. The unit is μ_B.

	This work	[6]	[33]	[44]
Co_1	0.64	0.60	0.77	
Co_2	0.41	0.38	0.40	
Co_3 triangle	0.29	0.25		
Co_3 linear	0.36	0.34	0.37	
Co_4	0.22	0.22		
Co_5 cross	0.27	0.27		
Overlayer	0.13		0.15	0.13

including geometry relaxation. The corresponding spin magnetic moments (per atom) are 2.00 μ_B, 1.96 μ_B, and 1.93 μ_B. We assume that the slower decrease of μ_{spin} with increasing cluster size obtained by Sabiryanov *et al* [26] is a consequence of the geometry relaxation.

As concerns magnetic moments induced in the Pt substrate, our results can be compared with the results of Lazarovits *et al* [33] for the 'extreme cases' of an ad-atom and of an overlayer. A reasonable agreement is found. For Pt atoms below a Co ad-atom, the total induced μ_{spin} is 0.39 μ_B in this work and 0.49 μ_B in [33] and the total induced μ_{orb} is 0.09 μ_B in this work and 0.11 μ_B in [33]. For Pt atoms below a Co overlayer, induced μ_{spin} is 0.19 μ_B in this work and 0.22 μ_B in [33], while the induced μ_{orb} is 0.05 μ_B in both studies. On the other hand, calculations of Sabiryanov *et al* suggest that the total μ_{spin} induced in Pt atoms below a Co ad-atom is as large as 1.65 μ_B [26] (with μ_{spin} for the first neighbours of the ad-atom being 0.14 μ_B [46]). The discrepancy between these values and the results of us and of Lazarovits *et al* [33] may be caused by the contraction of Co–Pt distances which is present in the work of Sabiryanov *et al* [26, 46]. However, one should also bear in mind that Sabiryanov *et al* relied on a supercell treatment of a 7-layer slab [46], which may lead to an overestimation of the influence of the Co ad-atom on more distant host atoms.

The average values for μ_{spin} and μ_{orb} decrease monotonically with the cluster size. This is partly because we focus on compact cluster shapes: if more open clusters such as linear Co_3 or a cross-shaped Co_5 were included (as in our earlier reports [14, 25]), oscillations would appear. Unsurprisingly, the bilayer Co_{10} cluster does not always fit into the sequence of monolayer clusters. This is mostly visible for induced moments in the Pt substrate, where the topmost three Co atoms are not in a direct contact with any substrate atom and hence practically do not contribute to Pt magnetism.

A similar monotonic reduction of the cluster magnetism with increasing cluster size was found in theoretical investigations of Fe clusters of 1–9 atoms on Ni surfaces [36, 47]. An

experimental investigation of small Fe clusters on Ni/Cu(001) based on XMCD sum rules yields a non-monotonic variation of μ_{spin} and μ_{orb} with cluster size. However, the error bars are quite large and a monotonic dependence is still consistent with the data [4]. In contrast to supported clusters, magnetic moments of free clusters exhibit a non-monotonic dependence on the cluster size within a small as well as an extended range of sizes [35, 48, 49]. It is thus possible that the substrate suppresses the tendency of magnetic moments to oscillate when the cluster size is varied. At the same time, the effect of different cluster shapes (spherical for free clusters, planar for supported clusters) cannot be ruled out.

Experimental data for μ_{orb} of Co clusters and for a Co overlayer on Pt(111) were obtained by Gambardella *et al* [6] by means of XMCD spectroscopy. As follows from figure 9, our calculation reproduces the general trend of μ_{orb} with cluster size but underestimates its magnitude. This is presumably due to correlation effects which are not fully incorporated in the LSDA framework. It was demonstrated that applying correlation corrections to the LSDA exchange–correlation potential by means of Brooks' OP formalism [34] improves the results in comparison with the observed orbital moments [6, 12, 50]. On the other hand, there are problems within the OP scheme which hinder its universal applicability [37].

Gambardella *et al* [6] also give an experimental estimate of the total (spin and orbital) magnetic moment induced in the Pt substrate below a Co ad-atom as $1.8 \pm 0.7\ \mu_{\mathrm{B}}$. This is considerably larger than our value of $0.48\ \mu_{\mathrm{B}}$. One should note, however, that several non-trivial assumptions had to be made by Gambardella *et al* in order to extract the magnetic moment of Pt from their data. XMCD measurements on a $Co_{13}Pt_3$ multilayer suggest that the total magnetic moment at the Pt interface layer is $0.69\ \mu_{\mathrm{B}}$ [19].

As concerns Co clusters on Au(111), experimental data are available only for large clusters. Weiss *et al* [17] investigated Co clusters of about 120 atoms on Au(111) microfacets via the XMCD sum rules analysis and estimated μ_{spin} as $1.7\ \mu_{\mathrm{B}}$ and μ_{orb} as $0.4\ \mu_{\mathrm{B}}$ per Co atom. Koide *et al* [16] applied a similar procedure to bilayer Co clusters of 400 atoms sandwiched between two Au(111) blocks and found that the spin and orbital magnetic moments of Co atoms are $\sim 2.1\ \mu_{\mathrm{B}}$ and $0.3\ \mu_{\mathrm{B}}$, respectively. These values are in the same range as the values we obtained for Co clusters on Au.

3.3. Density of states

Inspection of the density of states (DOS) further elucidates the mechanism with which the substrate affects magnetism of supported Co clusters. In accordance with the results of the previous section, one can assume that this mechanism will be the same for clusters and for overlayers. Therefore we focus on the technically simpler case of a Co overlayer and inspect how the DOS changes if a free-standing Co monolayer in vacuum is deposited onto a clean (111) surface of Pt, of Au with Pt geometry, and of Au. The geometry of the free-standing Co monolayer is always adjusted to the geometry of the substrate. The results are summarized in figure 10. For the sake of clarity we show the data only for the d states, which dominate in these systems. A broadening by a Lorentzian with a full width at half maximum of 0.25 eV was applied in order to suppress very fine DOS features.

As one would expect, the DOS at the Co sites broadens if a free-standing monolayer is deposited onto the substrate, because the states now get more hybridized and this way more delocalized. Likewise, decreasing the lattice constant of Au leads to a stronger hybridization and, consequently, to broader bands (compare the middle panels with the rightmost panels). It is also interesting to note that the changes in the DOS induced by the deposition of the Co overlayer are more pronounced at the substrate sites than at the Co sites. Similar trends were observed for a Co overlayer deposited on Pd(111) [43]. On the other hand, for a Co overlayer

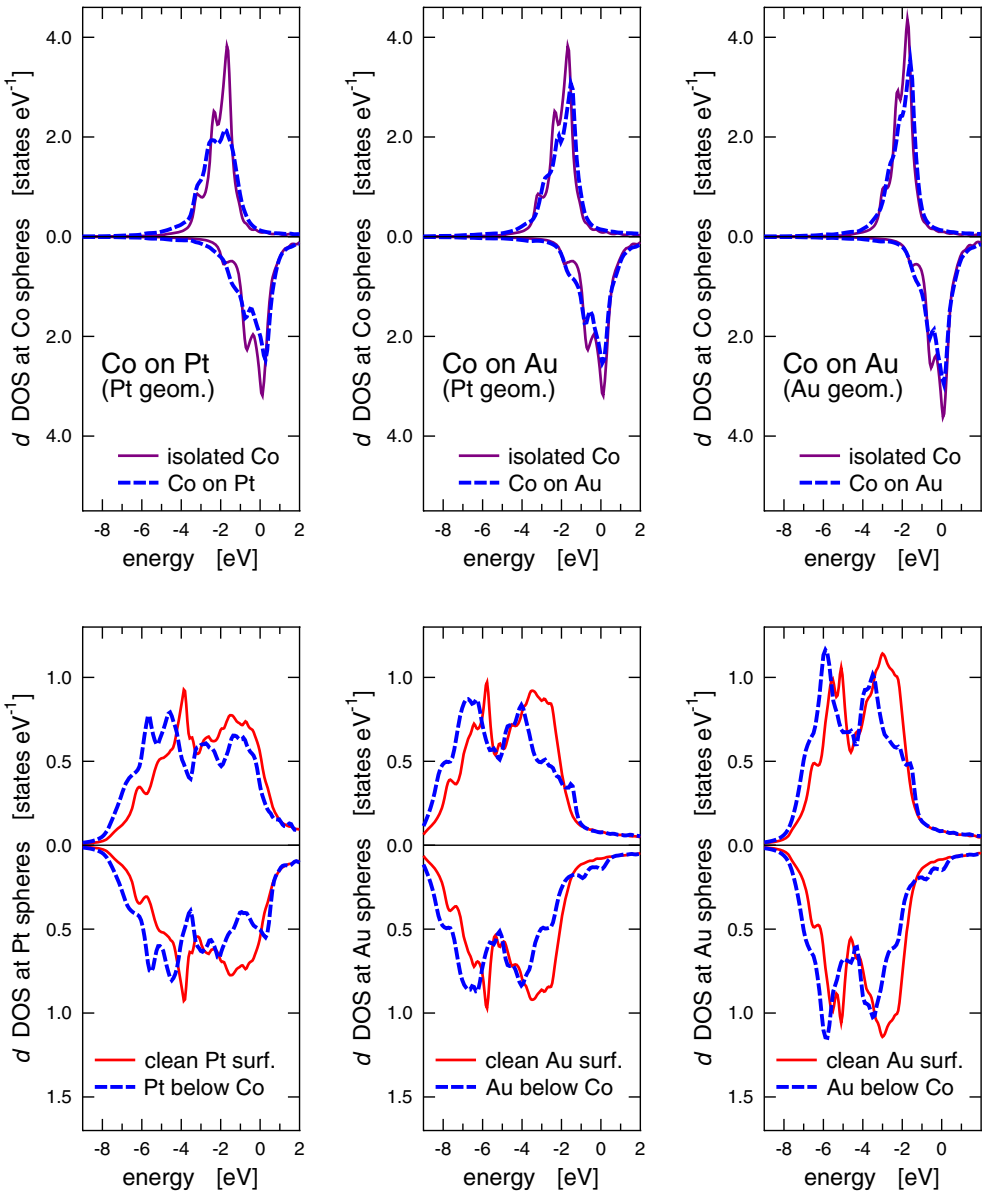

Figure 10. Upper panels: spin-polarized density of d states at Co atoms for a Co overlayer on Pt, on Au with Pt geometry, and on Au and for a corresponding free-standing Co monolayer. Lower panels: density of d states for the substrate atoms below the Co overlayer and for atoms at corresponding clean surfaces. The leftmost pair of panels represents Co on Pt, the middle pair represents Co on Au with Pt geometry, and the rightmost pair represents Co on Au.

on the W(110) surface, a big change of DOS with respect to a free-standing monolayer occurs at the Co sites [51].

A pure electronic structure effect can be observed by comparing the left panels of figure 10 with the middle panels (because these panels correspond to identical geometries). The first thing to note is that depositing the Co monolayer on Pt alters the DOS at Co sites more than

Table 3. Valence charges and μ_{spin} in Co spheres, decomposed according to the angular momentum. The first column of numbers represents a free-standing Co monolayer; the following columns show the amount by which these values change if the monolayer is deposited onto a clean Pt or Au surface. In all cases, the geometry matches the bulk Pt lattice. The charges are in fractions of an electron charge; the magnetic moments are in μ_{B}.

	Free-standing Co monolayer	Co on Pt (difference)	Co on Au with Pt geom. (difference)
$n_\uparrow + n_\downarrow$ (s)	0.71	−0.07	−0.08
$n_\uparrow + n_\downarrow$ (p)	0.38	0.21	0.19
$n_\uparrow + n_\downarrow$ (d)	7.60	0.06	0.09
$n_\uparrow$ (d)	4.79	0.01	−0.04
$n_\downarrow$ (d)	2.81	0.06	0.14
μ_{spin} (s)	0.01	−0.02	−0.02
μ_{spin} (p)	−0.02	−0.01	−0.02
μ_{spin} (d)	1.98	−0.05	−0.18

depositing it on Au—especially as concerns the majority states. This is plausible given the fact that the DOS of a free-standing monolayer has a substantially larger overlap with the DOS of Pt than with the DOS of Au, implying a stronger hybridization with the former [18]. On the other hand, a similar explanation cannot be applied to changes in the DOS at the Pt and Au sites, because in both cases the change is relatively large and it is by no means obvious which of them is the larger one. Apart from the effect of the DOS overlap, the stronger hybridization of Co with Pt than with Au may also be connected with the greater extent of the d states in Pt (the orbital radius of the 5d shell for atomic Pt is larger by 4% than for atomic Au [52]).

The magnitude of μ_{spin} is determined by the imbalance between occupied majority-spin and minority-spin states; hence it will be instructive to follow the transfer of spin-polarized charges. In order to highlight the effect of the electronic structure, we perform this analysis for systems with the same geometry. Table 3 shows the valence charges and spin magnetic moments accumulated in the s, p, and d states in a Co atomic sphere for a free-standing Co monolayer together with the *changes* of these quantities caused by depositing this monolayer either on Pt or on Au with Pt geometry. One can imagine such a process as disappearance of the vacuum region between the monolayer and the substrate. The charge contained in the vacuum region has to be transferred somewhere else, presumably primarily into the Co spheres and into the interface Pt or Au spheres. If follows from table 3 that most of the additional charge goes into the unpolarized p states. On the other hand, the decrease of μ_{spin} in the course of the deposition is realized mainly through changes of the occupancy of the d states. If Co atoms are deposited on Pt, a small amount of charge is added to the minority d states while the occupancy of the majority states remains unchanged. Consequently, only a relatively small decrease of μ_{spin} of the d states occurs that can be completely attributed to the increase of the d charge in Co spheres. On the other hand, a deposition of Co on Au causes not only a mild increase of the d charge but also a further redistribution of the d states from the majority to the minority spin orientation. Consequently, the decrease of $\mu_{\text{spin}}^{(\text{d})}$ is significantly larger than the amount of the transferred d charge.

The charge transfer in the substrate Pt or Au atoms is in some respect similar to the charge transfer in the Co atoms (table 4). The total occupancy of the s and of the d states in Pt or Au spheres practically does not change if a Co monolayer is deposited on the substrate. At the same time, the total occupancy of the p states increases by about 0.2 electrons. The appearance of a sizable μ_{spin} in Pt spheres is caused through a redistribution of d-electrons from states with minority to states with majority spin character.

Table 4. Differences between angular-momentum-decomposed charges and μ_{spin} of Pt or Au atoms below Co overlayers and on clean Pt and Au surfaces. The first column of numbers represents Pt; the second column represents Au with Pt geometry. The differences in μ_{spin} are in μ_{B}.

	Pt (difference)	Au with Pt geom. (difference)
$n_\uparrow + n_\downarrow$ (s)	0.02	0.01
$n_\uparrow + n_\downarrow$ (p)	0.20	0.21
$n_\uparrow + n_\downarrow$ (d)	0.02	0.00
$n_\uparrow$ (d)	0.11	0.01
$n_\downarrow$ (d)	−0.10	−0.01
μ_{spin} (s)	−0.01	−0.01
μ_{spin} (p)	−0.02	−0.02
μ_{spin} (d)	0.21	0.01

It is worth noting that the fact that clusters on Pt have a larger μ_{spin} than clusters on Au seems to be counterintuitive: the d band of a Co monolayer has a larger overlap with the d band of Pt than with the d band of Au, which suggests that the hybridization between the adsorbate and substrate bands is stronger for Co on Pt than for Co on Au and that, in turn, should imply that Co clusters on Pt will have a *smaller* μ_{spin} than Co clusters on Au. Such an intuitive argument can be applied for the Au and Ag substrates [37]; however, it apparently fails in our case. This might possibly be connected with the fact that different mechanisms are involved in suppressing the magnetism of initially free Co clusters by the Pt and Au substrates (simple increase of the number of electrons with the minority spin orientation in the case of Pt versus a redistribution of electrons from states with majority to minority spin orientation in the case of Au—see table 3).

Besides investigating how the DOS is influenced by the substrate, it is instructive to have a look at the influence of the cluster size. Figure 11 shows the DOS in Co spheres for supported clusters of 1, 2, and 7 atoms and also for a hypothetical bulk Co with the geometry of the underlying substrate (again, a Lorentzian broadening of 0.25 eV was applied). For the Co_7 cluster, the DOS at the central Co and at the Co at the edge of the hexagon is shown separately. One can see that for both substrates, the DOS curves get broader if the cluster size is increased and, simultaneously, a distinct fine structure appears. Similar trends were observed for finite Co wires on Pt(111) [33]. Interestingly, there is quite a substantial difference between the DOS of bulk Co and of the clusters we explore. In accordance with the situation for a Co overlayer, the DOS curves for clusters on Au are systematically more sharp than for clusters on Pt.

3.4. Exchange coupling

Exchange coupling constants J_{ij} were calculated on the basis of (2). As an illustration, the J_{ij} constants for Co_4 and Co_5 clusters supported by Au(111) are displayed in the lower diagrams of figure 12. The upper diagrams of figure 12 show the sum

$$J^{(i)} = \sum_{j \neq i} J_{ij}, \tag{4}$$

related to every atom. Such a quantity could be seen as the total strength by which a spin of atom i is held in its direction by interacting with all the other atoms.

Figure 12 illustrates a general rule that the coupling between nearest neighbours is nearly by an order of magnitude stronger than coupling between more distant atoms. We also found

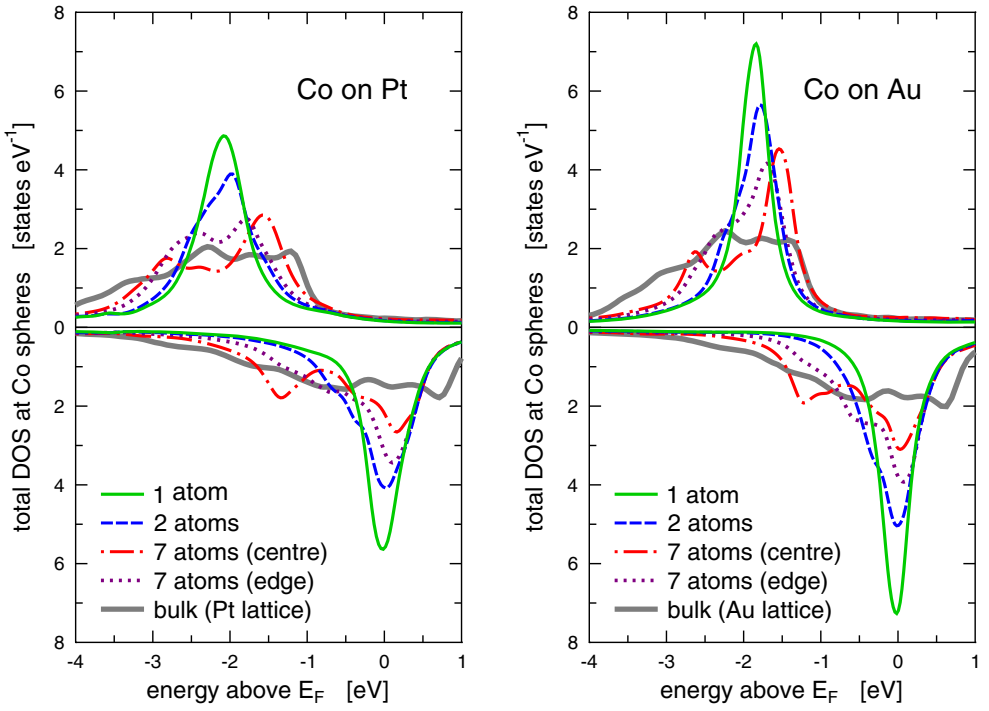

Figure 11. Total DOS for clusters of 1, 2, and 7 cobalt atoms on Pt (left panel) and on Au (right panel). Note that for the 7-atom cluster, the DOS curves for the central atom and for an edge atom are shown separately.

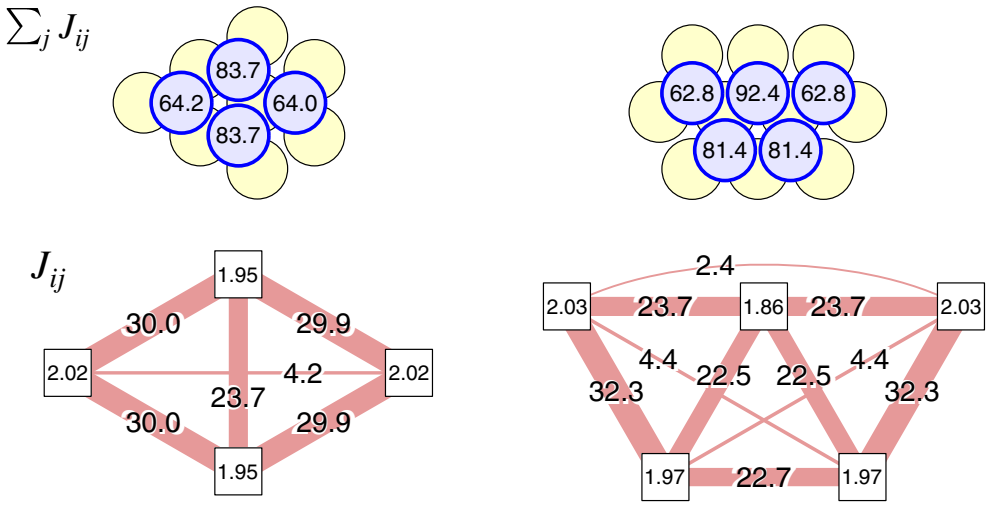

Figure 12. Exchange coupling in Co_4 and Co_5 clusters on Au(111). The lower diagrams depict pair-wise coupling constants J_{ij} (in meV); the thicknesses of the lines are proportional to J_{ij} and the numbers in the squares are local spin magnetic moments. The upper diagrams show, for each of the ith atom, the total coupling $J^{(i)}$ defined in (4) (in meV).

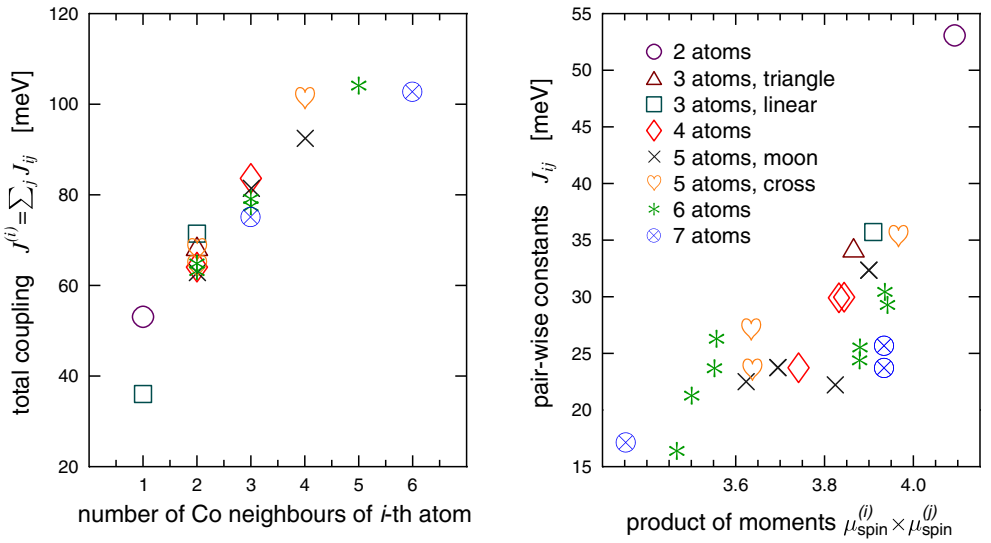

Figure 13. Left panel: total coupling $J^{(i)}$ in Co clusters of 2–7 atoms on Au(111) plotted against the number of Co neighbours of the ith atom. Right panel: pair-wise coupling constants J_{ij} between atoms in the same systems, plotted against the product of spin magnetic moments of the ith and the jth atom. The size and the shape of each cluster are identified in the legend.

that, for all the clusters we investigated, the J_{ij} constants are always positive. The only exception is the coupling between the most distant atoms in the Co_{10} cluster on Au (i.e., between the two edge atoms which lie in the opposite directions from the centre), where the J_{ij} constant is -1.1 meV.

Intuitively, one can expect that the total coupling $J^{(i)}$ of the ith atom will be proportional to its coordination number—more neighbours means more terms in the sum in (4). Figure 12 illustrates this tendency for two cluster sizes. A systematic exploration of the dependence of $J^{(i)}$ on the coordination number for a whole range of sizes of monolayer clusters on Au(111) is performed in the left graph of figure 13. One can see that the deviations from the suggested correlation are not large—although signs of saturation appear for coordination numbers bigger than four.

The coupling constants J_{ij} determined by (1) and (2) already contain $\mu_{\rm spin}$ of the coupled atoms. If the effects of the cluster size and of the local coordination were negligible, the nearest-neighbour J_{ij} should be proportional to the product of magnetic moments of the ith and jth atom. Deviations from this proportionality can be thus seen as a measure of how finite cluster size affects the exchange coupling. Therefore, we display in the right graph of figure 13 the coupling constants J_{ij} between neighbouring atoms in Co clusters supported by Au(111) as a function of the product $\mu_{\rm spin}^{(i)} \times \mu_{\rm spin}^{(j)}$. One can see that although larger magnetic moments generally lead to a larger coupling, the spread of the J_{ij}-values around the linear relation is significant. This can be viewed as a demonstration that using bulk coupling constants for studying finite-temperature cluster magnetism would be inappropriate.

The data presented in figures 12 and 13 represent results for Co clusters on Au(111). Focusing on the Pt substrate would lead to similar conclusions as for the Au substrate: just the numerical values of the coupling constants would be larger. Generally, when going from one substrate to another, one can expect that the exchange coupling will be affected by the magnitude of $\mu_{\rm spin}$ and by interatomic distances. In order to have a quantitative measure, we

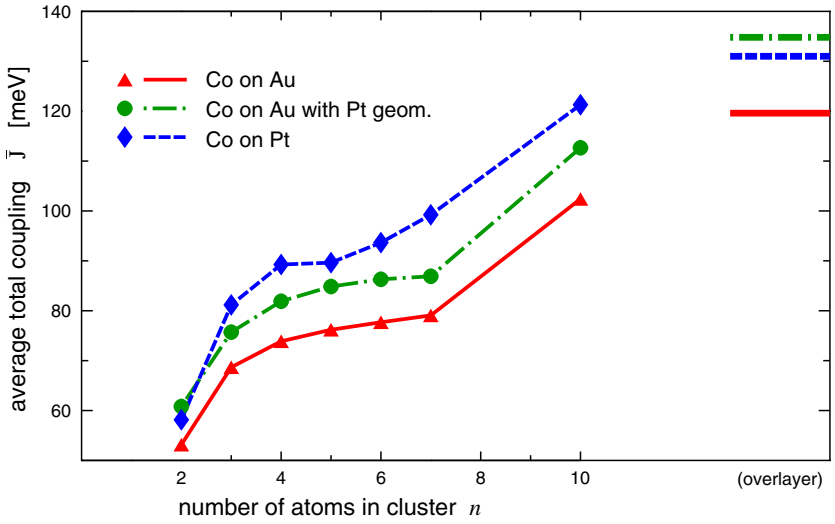

Figure 14. Average total coupling $\bar{J}$ for atoms in compact Co clusters on Au, on Au with Pt geometry, and on Pt. Corresponding values for Co overlayers are indicated at the right border of the graph.

investigate the average total couping $\bar{J}$:

$$\bar{J} \equiv \frac{1}{n}\sum_i J^{(i)} = \frac{1}{n}\sum_i \sum_{j\neq i} J_{ij}. \tag{5}$$

The dependence of $\bar{J}$ on the size of Co clusters on Pt(111), on Au(111) with Pt geometry, and on Au(111) is shown in figure 14. Data for Co overlayers are shown as well (in these cases, $\bar{J}$ is identical to $J^{(i)}$ for any i). For clusters on the Pt substrate, about 95% of the $\bar{J}$-value comes from the Co–Co coupling and the remaining 5% from the Co–Pt coupling. For clusters on the Au substrate, the Co–Au coupling constitutes less than 1% of $\bar{J}$.

Unsurprisingly, $\bar{J}$ is largest for the Pt substrate, for which the Co magnetic moments are larger and the interatomic distances are smaller than for the other substrates. A competition between both trends occurs when comparing clusters on Au and on Au with Pt geometry: decreasing the lattice constant from the Au value to the Pt value leads to a contraction of interatomic distances and thus to an enhancement of $\bar{J}$ and, at the same time, it leads also to a decrease of μ_{spin} of Co atoms and thus to a reduction of $\bar{J}$. As can be seen in figure 14, the effect of decreasing the interatomic distances prevails. An interesting transposition of $\bar{J}$-values occurs at both ends of our cluster size range: the exchange coupling in the Co_2 cluster and in the Co overlayer is weaker on Pt than on Au with Pt geometry, even though the magnetic moments are larger for the former substrate.

It follows from figure 14 that $\bar{J}$ increases monotonically with the cluster size. This is plausible: increasing the cluster size means increasing the average coordination number, which in turn means increasing the coupling. Note that if other than compact shapes were included in figure 14, one would get a non-monotonic behaviour: $\bar{J}$ of a linear Co_3 cluster is smaller than $\bar{J}$ of a triangular cluster; similarly $\bar{J}$ of a cross-shaped Co_5 cluster is smaller than $\bar{J}$ of a half-moon cluster. For atoms in overlayers, the sums in (4) and (5) formally include an infinite number of terms, so it is not surprising that $\bar{J}$ for overlayers is larger than for clusters. One gets even larger values of $\bar{J}$ for a hypothetical bulk Co with an fcc Pt lattice (168 meV) or with an fcc Au lattice (158 meV).

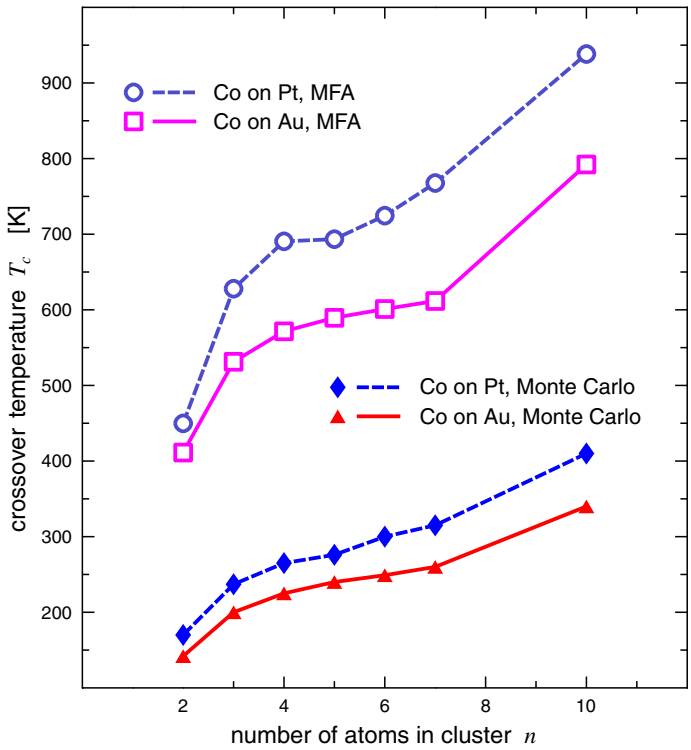

Figure 15. Dependence of T_c of compact Co clusters on Au(111) and Pt(111) on the cluster size.

Nearest-neighbour coupling constants J_{ij} for Co dimer and trimer on Pt(111) were published by Sabiryanov *et al* [26]. Their values (29 and 27 meV for Co_2 and Co_3, respectively) are smaller than the values obtained in this work (55 and 39 meV). The study of Sabiryanov *et al* involves Co atoms which have, because of geometry relaxation, about 10% smaller μ_{spin} and about 20% smaller interatomic distances than Co atoms treated in this work. Assuming that J_{ij} is approximately linear in the square of μ_{spin} (figure 13) and inversely proportional to the cube of the interatomic distance [53], one can crudely estimate that J_{ij} should be about 60% *larger* in the study of Sabiryanov *et al* than in this work, contrary to what really happens. A possible source of this discrepancy might be an interference between adjacent supercells in the formalism employed by Sabiryanov *et al* [26, 46]. At the same time, the influence of the ASA used by us cannot be ruled out. It is worth noting that when applying the above scaling to $\bar{J}$ for bulk fcc Co presented in this work (with either Pt or Au lattice) and for bulk hcp Co provided by Sabiryanov *et al* [26] (175 meV), one gets a reasonable agreement between the computed and 'scaled' values (better than 10%).

3.5. Crossover temperatures

Figure 15 shows the crossover temperature T_c as a function of the size of compact Co clusters for Pt(111) and Au(111) substrates as obtained from our Monte Carlo simulations. For comparison, we present also T_c calculated from the relation

$$T_c^{MFA} = \frac{2}{3}\frac{1}{k_B}\bar{J}, \tag{6}$$

which is an extension of the mean-field approximation from the bulk case to finite clusters.

A tendency of T_c to increase with increasing cluster size is obvious. Similarly as in the case of magnetic moments and average coupling, the dependence of T_c on the cluster size would not be monotonic if open shapes were included. In all cases, T_c of our clusters is well below the theoretical Curie temperature of bulk fcc Co as evaluated either using a random phase approximation (1311 K) or using a mean-field approximation (1645 K) [53].

The crossover temperature of clusters on the Pt substrate is higher than that of clusters on the Au substrate. This is consistent with the trends of average coupling constants $\bar{J}$, as reflected by T_c^{MFA} in figure 15. On the other hand, a closer look at figure 15 reveals that T_c is not simply proportional to T_c^{MFA} and hence not to $\bar{J}$.

4. Summary

Our fully relativistic *ab initio* calculations suggest that magnetic moments of small Co clusters on Pt(111) and on Au(111) decrease monotonically with increasing cluster size but always remain enhanced with respect to the bulk or to a Co overlayer. Spin magnetic moments of Co clusters are larger for the Pt substrate than for the Au substrate, while the reverse is true for orbital magnetic moments. The local μ_{spin} and μ_{orb} of Co atoms generally increase if the number of Co neighbours decreases. Pt atoms which are nearest neighbours of any Co atom have an induced μ_{spin} of 0.07–0.14 μ_B and induced μ_{orb} of 0.02–0.03 μ_B, while analogous Au atoms have a small negative induced μ_{spin} ($\lesssim$0.02 μ_B) and practically zero μ_{orb}. Pair-wise exchange coupling between neighbouring Co atoms is only approximately proportional to the product of their magnetic moments. The total exchange coupling of any atom in a cluster generally increases if its coordination number increases. On average, the exchange coupling is larger between atoms on Pt than between atoms on Au. The crossover temperature predicted by Monte Carlo simulations increases with cluster size monotonically and is larger for clusters on Pt than for clusters on Au.

Acknowledgments

This work was supported by the grant 202/04/1440 of the Grant Agency of the Czech Republic. The research in the Institute of Physics AS CR was supported by the project AV0Z-10100521 of Academy of Sciences of the Czech Republic. Support by the Deutsche Forschungsgemeinschaft within the Schwerpunktprogramm 1153 'Cluster in Kontakt mit Oberflächen: Elektronenstruktur und Magnetismus' and by the BMBF project 05KS4WMB/2 is gratefully acknowledged.

References

[1] Edmonds K W, Binns C, Baker S H, Thornton S C, Norris C, Goedkoop J B, Finazzi M and Brookes N B 1999 *Phys. Rev.* B **60** 472
[2] Ohresser P, Ghiringhelli G, Tjernberg O, Brookes N B and Finazzi M 2000 *Phys. Rev.* B **62** 5803
[3] Ohresser P, Brookes N B, Padovani S, Scheurer F and Bulou H 2001 *Phys. Rev.* B **64** 104429
[4] Lau J T, Föhlisch A, Nietubyc R, Reif M and Wurth W 2002 *Phys. Rev. Lett.* **89** 057201
[5] Gambardella P, Dhesi S S, Gardonio S, Grazioli C, Ohresser P and Carbone C 2002 *Phys. Rev. Lett.* **88** 047202
[6] Gambardella P, Rusponi S, Veronese M, Dhesi S S, Grazioli C, Dallmeyer A, Cabria I, Zeller R, Dederichs P H, Kern K, Carbone C and Brune H 2003 *Science* **300** 1130
[7] Wildberger K, Stepanyuk V S, Lang P, Zeller R and Dederichs P H 1995 *Phys. Rev. Lett.* **75** 509
[8] Stepanyuk V S, Hergert W, Rennert P, Wildberger K, Zeller R and Dederichs P H 1997 *J. Magn. Magn. Mater.* **165** 272
[9] Stepanyuk V S, Hergert W, Rennert P, Wildberger K, Zeller R and Dederichs P H 1999 *Phys. Rev.* B **59** 1681
[10] Izquierdo J, Bazhanov D I, Vega A, Stepanyuk V S and Hergert W 2001 *Phys. Rev.* B **63** 140413(R)
[11] Felix-Medina R, Guirado-Lopez R, Dorantes-Davila J and Pastor G M 2000 *J. Appl. Phys.* **87** 4894

[12] Nonas B, Cabria I, Zeller R, Dederichs P H, Huhne T and Ebert H 2001 *Phys. Rev. Lett.* **86** 2146
[13] Lazarovits B, Szunyogh L and Weinberger P 2002 *Phys. Rev.* B **65** 104441
[14] Minár J, Bornemann S, Šipr O, Polesya S and Ebert H 2006 *Appl. Phys.* A **82** 139
[15] Dürr H A, Dhesi S S, Dudzik E, Knabben D, van der Laan G, Goedkoop J B and Hillebrecht F U 1999 *Phys. Rev.* B **59** R701
[16] Koide T, Miauchi H, Okamoto J, Shidara T, Fujimori A, Fukutani H, Amemiya K, Takeshita H, Yuasa S, Katayama T and Suzuki Y 2001 *Phys. Rev. Lett.* **87** 257201
[17] Weiss N, Cren T, Epple M, Rusponi S, Baudot G, Rohart S, Tejeda A, Repain V, Rousset S, Ohresser P, Scheurer F, Bencok P and Brune H 2005 *Phys. Rev. Lett.* **95** 157204
[18] Guo G Y and Ebert H 1995 *Phys. Rev.* B **51** 12633
[19] Wilhelm F, Poulopoulos P, Scherz A, Wende H, Baberschke K, Angelakeris M, Flevaris N K, Goulon J and Rogalev A 2003 *Phys. Status Solidi* a **196** 3
[20] Wilhelm F, Angelakeris M, Jaouen N, Poulopoulos P, Papaioannou E T, Mueller C, Fumagalli P, Rogalev A and Flevaris N K 2004 *Phys. Rev.* B **69** 220404(R)
[21] Vosko S H, Wilk L and Nusair M 1980 *Can. J. Phys.* **58** 1200
[22] Ebert H 2000 *Electronic Structure and Physical Properties of Solids* (*Lecture Notes in Physics* vol 535) ed H Dreyssé (Berlin: Springer) p 191
[23] Weinberger P 1990 *Electron Scattering Theory for Ordered and Disordered Matter* (Oxford: Oxford University Press)
[24] Zeller R, Dederichs P H, Újfalussy B, Szunyogh L and Weinberger P 1995 *Phys. Rev.* B **52** 8807
[25] Bornemann S, Minár J, Polesya S, Mankovsky S, Ebert H and Šipr O 2005 *Phase Transit.* **78** 701
[26] Sabiryanov R F, Cho K, Larsson M I, Nix W D and Clemens B M 2003 *J. Magn. Magn. Mater.* **258/259** 365
[27] Papanikolaou N, Nonas B, Heinze S, Zeller R and Dederichs P H 2000 *Phys. Rev.* B **62** 11118
[28] Gusso M 2006 *J. Phys.: Condens. Matter* **18** 1211
[29] Liechtenstein A I, Katsnelson M I, Antropov V P and Gubanov V A 1987 *J. Magn. Magn. Mater.* **67** 65
[30] Binder K 1997 *Rep. Prog. Phys.* **60** 487
[31] Landau D P and Binder K 2000 *A Guide to Monte Carlo Simulations in Statistical Physics* (Cambridge: Cambridge University Press)
[32] Polesya S, Šipr O, Bornemann S, Minár J and Ebert H 2006 *Europhys. Lett.* **74** 1074
[33] Lazarovits B, Szunyogh L and Weinberger P 2003 *Phys. Rev.* B **67** 24415
[34] Brooks M S S 1985 *Physica* B **130** 6
[35] Šipr O, Košuth M and Ebert H 2004 *Phys. Rev.* B **70** 174423
[36] Mavropoulos P, Lounis S, Zeller R, Dederichs P H and Blügel S 2006 *Appl. Phys.* A **82** 103
[37] Cabria I, Nonas B, Zeller R and Dederichs P H 2002 *Phys. Rev.* B **65** 054414
[38] Pick Š, Stepanyuk V S, Baranov A N, Hergert W and Bruno P 2003 *Phys. Rev.* B **68** 104410
[39] Shick A B, Máca F and Oppeneer P M 2004 *Phys. Rev.* B **69** 212410
[40] Máca F, Shick A B, Redinger J and Oppeneer P M 2006 *Czech. J. Phys.* **56** 51
[41] Pick Š, Stepanyuk V S, Klavsyuk A L, Niebergall L, Hergert W, Kirschner J and Bruno P 2004 *Phys. Rev.* B **70** 224419
[42] Nogueira R N and Petrilli H M 1999 *Phys. Rev.* B **60** 4120
[43] Wu R, Li C and Freeman A J 1991 *J. Magn. Magn. Mater.* **99** 71
[44] Komelj M, Ederer C, Davenport J W and Fähnle M 2002 *Phys. Rev.* B **66** 140407(R)
[45] Cabria I, private communication
[46] Sabiryanov R F, Larsson M I, Cho K, Nix W D and Clemens B M 2003 *Phys. Rev.* B **67** 125412
[47] Martínez E, Longo R C, Robles R, Vega A and Gallego L J 2005 *Phys. Rev.* B **71** 165425
[48] Billas I M L, Châtelain A and de Heer W A 1994 *Science* **265** 1682
[49] Wan X, Zhou L, Dong J, Lee T K and Wang D 2004 *Phys. Rev.* B **69** 174414
[50] Ebert H, Bornemann S, Minár J, Košuth M, Šipr O, Dederichs P H, Zeller R and Cabria I 2005 *Phase Transit.* **78** 71
[51] Spišák D and Hafner J 2004 *Phys. Rev.* B **70** 014430
[52] Mann J B 1968 *Los Alamos Scientific Laboratory Report* LA-3691
[53] Pajda M, Kudrnovský J, Turek I, Drchal V and Bruno P 2001 *Phys. Rev.* B **64** 174402